ARTICLE

OPEN

Check for updates

Synthesis of ^{14}C-labelled polystyrene nanoplastics for environmental studies

Maya Al-Sid-Cheikh[1,6]✉, Steven J. Rowland[2], Ralf Kaegi[3], Theodore B. Henry[4], Marc-André Cormier[5] & Richard C. Thompson[1]

Available analytical methods cannot detect nanoplastics at environmentally realistic concentrations in complex matrices such as biological tissues. Here, we describe a one-step polymerization method, allowing direct radiolabeling of a sulfonate end-capped nano-sized polystyrene (nPS; proposed as a model nanoplastic particle representing negatively charged nanoplastics). The method, which produces nanoplastics trackable in simulated environmental settings which have already been used to investigate the behavior of a nanoplastic in vivo in a bivalve mollusc, was developed, optimized and successfully applied to synthesis of ^{14}C-labeled nPS of different sizes. In addition to a description of the method of synthesis, we describe the details for quantification, mass balance and recovery of the labelled particles from complex matrices offered by the radiolabelling approach. The radiolabeling approach described here, coupled to use of a highly sensitive autoradiographic method for monitoring nanoplastic body burden and distributions, may provide a valuable procedure for investigating the environmental pathways followed by negatively charged nanoplastics at low predicted environmental concentrations. Whether the behaviour of the synthetic nPS manufactured here, synthesised using a very common initiator, represents that of manufactured nPS found in the environment, remains to be seen.

[1] School of Biological and Marine Science, University of Plymouth, Drake Circus, Plymouth PL4 8AA, UK. [2] School of Geography, Earth and Environmental Sciences, University of Plymouth, Drake Circus, Plymouth PL4 8AA, UK. [3] Eawag, Swiss Federal Institute of Aquatic Science and Technology, Überlandstrasse 133, P.O. Box 611, 8600 Dübendorf, Switzerland. [4] Institute of Life and Earth Sciences, Heriot-Watt University, John Muir Building, Edinburgh EH14 4AS, UK. [5] Department of Earth Sciences, University of Oxford, South Parks Road, Oxford OX1 3AN, UK. [6] Present address: Department of Chemistry, University of Surrey, Stag Hill, Guildford GU2 7XH, UK. ✉email: m.al-sid-cheikh@surrey.ac.uk

Paradigms for assessing the potential environmental impacts of manufactured nanomaterials have been eloquently described[1]. Among such nanomaterials, plastic particles exhibiting at least one dimension below 1 µm (i.e. so-called nanoplastics; NPs) have been reported to have the potential to become the most hazardous component of marine plastic litter[2,3]. NPs are suspected to be released into the environment directly from their addition to a range of commercial products[4,5] and by fragmentation of larger pieces of plastic litter[2,6–9]. The potential impacts of the sizes of particles (i.e. nano-sizes) on their degradation, uptake and biodistribution in organisms have been the subject of several studies[3,10]. Recently, the use of a synthetic ^{14}C-radiolabeled nanopolystyrene (nPS) either to study NP degradation in water and air[9] or, when coupled with autoradiography, to monitor the biodistribution of an NP in a bivalve mollusc has been described[11]. Although a multistep method for producing ^{14}C-nPS from cinnamic acid via styrene has been reported[9], the details of the one-step synthesis of ^{14}C-nPS used in the biodistribution study[9] have not. Therefore, here we show these details, including the effects of controlling factors on the production of nPS particles with a range of sizes suitable for deployment in simulated environmental studies at low predicted NP concentrations. The resultant method using ^{14}C-styrene is simple and robust, requiring only minimal reagents, a 20 mL vial sealed with a rubber septum, a magnetic stirrer and an oil bath. We review the advantages of using synthetic radiolabelled particles in environmental experiments.

The NP concentrations to which organisms are predicted to be exposed in natural and technical environments are very low (between ca. 1 pg L^{-1} and ca 20 µg L^{-1})[12]. It is therefore important that the possible in vivo biodistributions and toxicokinetics of NP are explored using approaches which offer sufficiently low NP limits of detection. However, deployment of the most common analytical methods to study the fate and effects of commercially available NP may mean they are not detectable at environmentally realistic concentrations in complex matrices, such as biological tissues. Most current studies investigating bioaccumulation and effects of NP in organisms such as mussels[13], oysters[13], algae[14], copepods[15], *Daphnia*[16] and fish[17] have been carried out with commercial fluorescent or functionalized NP, with experimental exposure concentrations two to seven orders of magnitude higher than those predicted to occur in the environment[12]. For fluorescent NP these high limits of detection are due to factors such as high background signals, poor resolution due to autofluorescence, quenching of fluorescence[18] and leaching of the fluorescent label[19]. These factors limit the applications of commercial NP for providing reliable and quantitative data. However, it is now possible to gather information on the quantitative biodistribution and toxicokinetics of NP particles in environmentally realistic scenarios using radiolabelled ^{14}C-NP[9,11].

To produce ^{14}C-NP of different sizes, we modified and improved the synthesis methods used for non-radiolabelled nPS previously[18,19]. One challenge of the synthesis of radioactive nPS, compared to that of unlabelled material, is the high cost of radioactive styrene monomer. Tian et al.[9] overcame this somewhat by conducting a multistep synthesis of [14]C nPS from labelled cinnamic acid. An alternative, used herein, was to improve the efficiency such that reactions using <10 mg of styrene monomer and very small volumes of reagents (<10 mL) could be conducted. Since the use for environmental studies also requires nPS with minimal- and ideally no co-products (e.g. styrene monomer, surfactants), the final method comprised a one-step polymerisation process using either 2 wt% of surfactant (for small, target 20 nm) or no surfactant (for large, target 250 nm) particles, followed by purification by dialysis. To optimise the

method of production with minimal amounts of reagents, we examined the effects of the changes in the concentrations of the most commercially used initiator (here sodium persulfate, KPS), surfactant (sodium dodecyl sulfate, SDS), and of sodium hydroxide. The use of KPS gives a negative surface charge to the particles, which may make them a good model for studies in environmental settings. In fact, such negative charges are likely to occur on particles in environmental media by the sorption of fulvic and humic acids at relevant pH values[20]. As in industrial settings, other initiators could be considered. Indeed, it would be interesting in future to investigate the behaviour of primary NPs with different surface chemistries in environmental contexts using the approach discussed in this study.

Results and discussion

Radioabelling strategy. As described in Fig. 1, the reaction was initiated by formation of a KPS radical at 65–75 °C in water (Fig. 1a, 1). The presence of such a radical initiated the formation of styrene radicals (Fig. 1a, 2), which created a polymerisation cascade (Fig. 1a, 2).

In this study, nominal 20 nm nPS was formed by the polymerisation of ^{14}C-styrene in the presence of SDS in an emulsion of water and hexane (7:3), mixed by mechanical shear (i.e. 150 r.p.m.). SDS reduced the surface tension of water, producing nano-sized particles of polystyrene, defined by micro-emulsions with dispersed domain diameters varying from 1 to 100 nm[21]. Thus, in the presence of SDS, nPS monomers nucleated inside SDS-micelles swollen with the input of monomers[22], reaching sizes up to 100 nm (Fig. 1b). In the absence of surfactants, the nucleation is thought to occur by the collapsing of water-insoluble polymer chains, forming precursor particles[22]. These unstable precursors (i.e. solidified nanoparticles of ~10 nm[23]) that become monomers of larger particles are believed to aggregate until they produce enough surface charge to be individually stable (Fig. 1c). Such aggregates can then swell by incorporating more monomers, forming mature particles (up to ~500 nm)[24]. Both sizes of particles are colloidally stabilised electrostatically by the persulfate end groups of the initiator at the surface of the particles[25].

Syntheses optimisation. Syntheses of both sizes of non-labelled nPS (i.e. 20 and 250 nm) were also performed with ^{12}C-styrene in order to provide materials for transmission electron microscopy (TEM) measurements. (Safety regulations prevented use of radioactive nPS for TEM investigations.) Results from TEM analyses indicated that the size of the nominally 20 nm polystyrene particles (nPS$_{20}$) remained fairly constant, even when the concentrations of styrene or SDS were changed substantially (Fig. 2a, c). Particles reached an overall average size of 20.6 ± 4.9 nm (n > 100) over the different styrene concentrations: 24.8 ± 12.8 (n > 100) with changes in KPS and 21.6 ± 3.0 nm (n > 100) with changes in SDS concentrations. Interestingly, at the highest KPS concentration of 50 mM (Fig. 2b), the particles showed a tendency to reach larger sizes (47.5 ± 9.3 nm), which might be due to the high concentrations of initiator, perhaps initiating more polymerisation and increasing the aggregation of nucleus per drop of monomer. Also, according to the results of dynamic light scattering (DLS) measurements, particles formed at low styrene concentrations were estimated at about 70 nm, whereas they were measured at about 20 nm by TEM. Such results show that the particles probably clustered when produced under such conditions.

The larger nPS particles were produced using a technique employed industrially to produce polymeric particles with large diameters (i.e. d > 100 nm) and narrow size distributions[26]. The
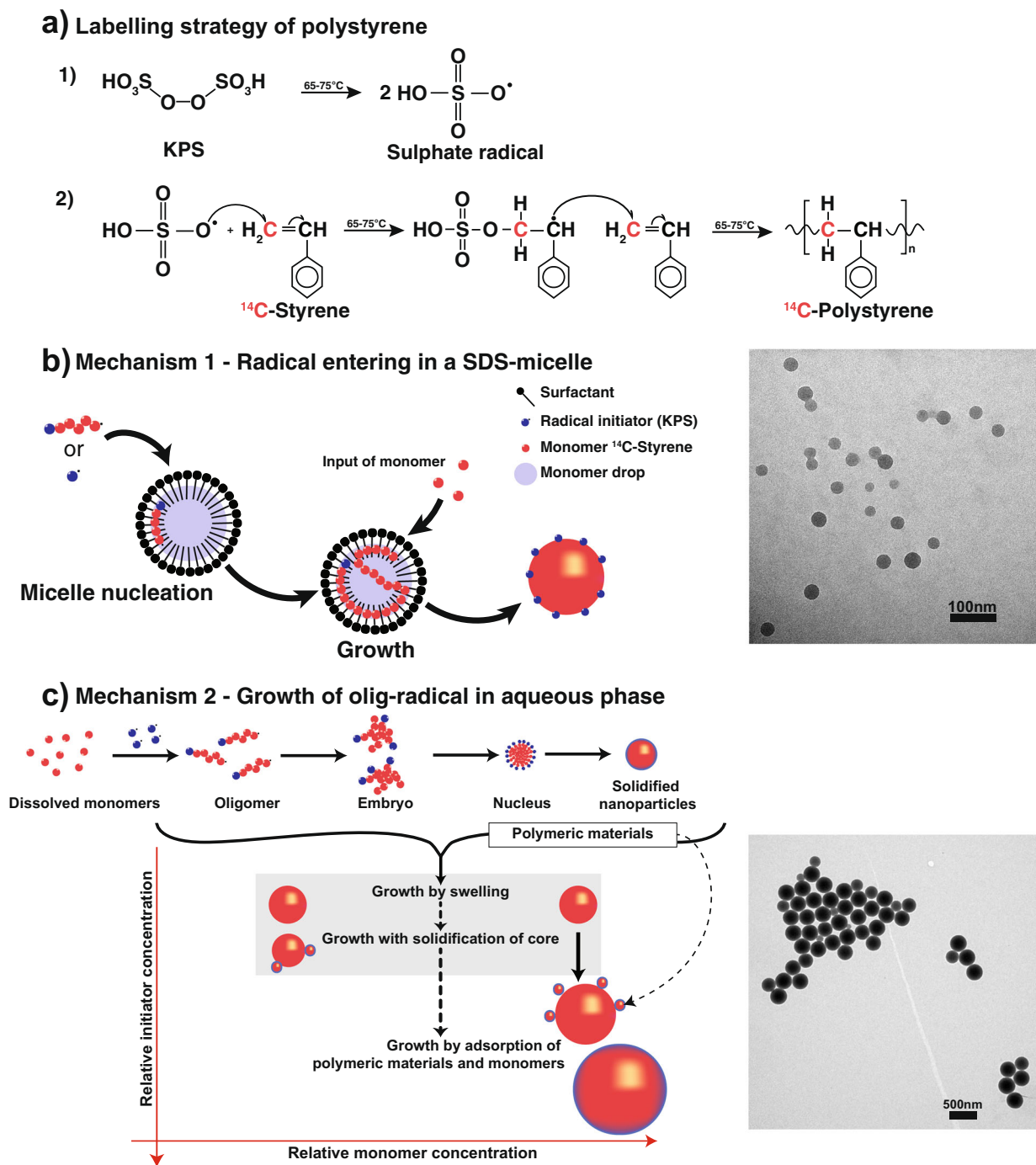
Fig. 1 Intrinsic radiolabelling strategy. a Proposed labelling strategy of polystyrene from macromolecule to nanoparticles. (1) Initiator potassium persulfate (KPS) produces water soluble SO_4^- radical which must first polymerise in the water phase until becoming sufficiently hydrophobic to enter into the organic phase[32] to (2) initiation of ^{14}C-styrene radical for the polymerisation, propagation and termination[33]. Overview of the mechanisms forming: **b** small ^{14}C-nPS (target 20 nm) with surfactant in the system according to Smith–Ewart–Harkins theory[33] for unlabelled nPS; **c** large ^{14}C-labelled nPS (target 250 nm) in the aqueous phase as per the method of Yamamoto et al.[23] for unlabelled nPS. The large red spheres with a blue outer line represent aggregates of solidified smaller nanoparticle monomers. Red carbon atoms are ^{14}C-labelled (i.e. styrene [methylene-^{14}C]); blue indicates the radical initiator (KPS); purple circles are monomer drops; black pins represent surfactant. Transmission electron microscopy images of particles synthesised are displayed to the right of the mechanisms shown in **b** and **c**.

syntheses of these larger polystyrene particles (nominally nPS$_{250}$) showed that, over all the synthesis conditions tested, particles reached minimum sizes of 198 ± 43 nm, with 1 wt% styrene, as measured by TEM (Fig. 2d), but the average size also increased with increases in the concentration of KPS, up to 451.9 ± 186.8 nm (Fig. 2e) where the concentration of initiator (i.e. KPS)

promoted particle growth. The absence of surfactant in the syntheses of nPS$_{250}$ simplified the synthesis (i.e. no nitrogen atmosphere was needed).

Particles purification and characterisation. To avoid potential toxicological effects associated with SDS and unreacted
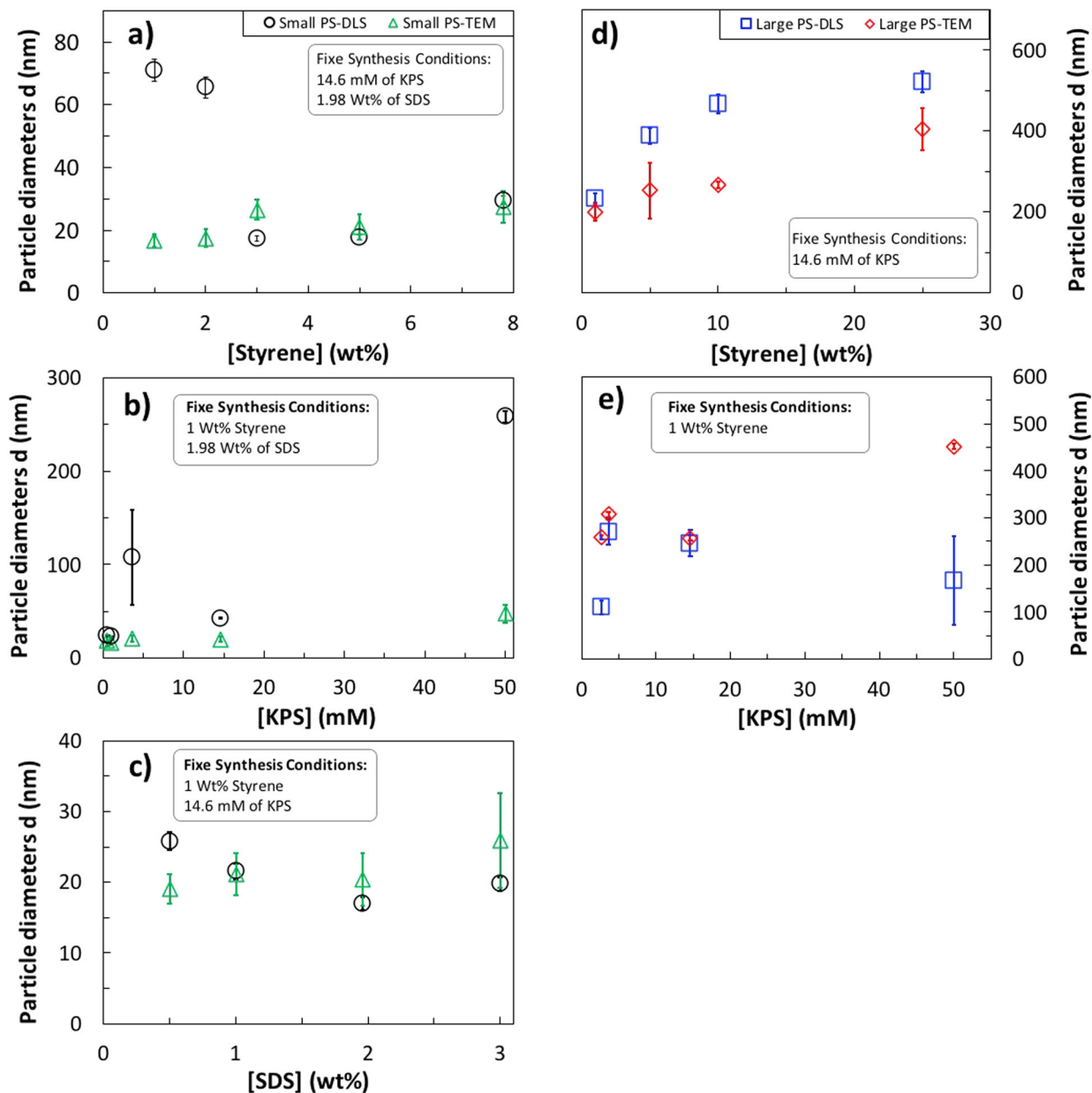
Fig. 2 Optimisation of nPS syntheses in small volume. Size optimisation for the synthesis of nPS with a targeted size of 20 nm (**a–c**) and 250 nm (**d, e**) for variations of styrene, sodium dodecyl sulfate (SDS) and potassium persulfate (KPS) concentrations (wt% in w/w or mM). Particles in **b**, **c** and **e** were synthesised with 1% styrene. Black circles and blue squares represent data from dynamic light scattering (DLS) measurements and green triangles and red diamonds represent data from TEM measurements. The error bars represent the size standard deviation of uncertainty (2 sigmas) for each synthesis. Complete data and images are available in the Supplementary Figures and Tables.

chemicals (e.g. KPS and styrene monomer), purification by dialysis (exclusion size of membrane 30,000 g mol^{-1}, ca. $d = 2$ nm[27]) was performed until the conductivity of the surrounding water remained constant at a value of <1.5 µS cm^{-1} and ^{14}C counting reached background levels. Interestingly, keeping a KPS concentration below ~15 mM also allowed the preparation of particles with a narrow size distribution (i.e. a range of SD < 30 nm), which is uncommon in systems with no stabilising agent[24–28].

Besides the potential to produce NP for ecotoxicological studies, the strength of the method lies in its simplicity and robustness: the method corresponds to a one-step synthesis and requires only a 20 mL vial sealed with a rubber septum, a magnetic stirrer and an oil bath.

Following the TEM measurements of unlabelled styrene and optimisation of the reaction conditions (Fig. 2), nPS particles were produced using ^{14}C-styrene. Based on the activity measured in the reaction medium before and after synthesis and purification, the yields for 'small' and 'large' nPS were estimated at 98% and 99%, respectively. A specific activity of 0.16 MBq ^{14}C/mgC NP was found after synthesis and the nPS suspensions were stable for weeks (i.e. no deposition was observed). The particles were stabilised by the negative charges of the sulfonic groups (i.e. derived from the initiator). At pH 6 in sodium chloride (5 mM), their ξ-potentials were −129 ± 10 and −83.6 ± 11.9 mV, while their sizes, as determined by DLS performed on a dedicated Zetasizer (Malvern Panalytic®), were 146 ± 29 and 275.9 ± 55 nm, for nominal ^{14}C-nPS$_{20}$ and
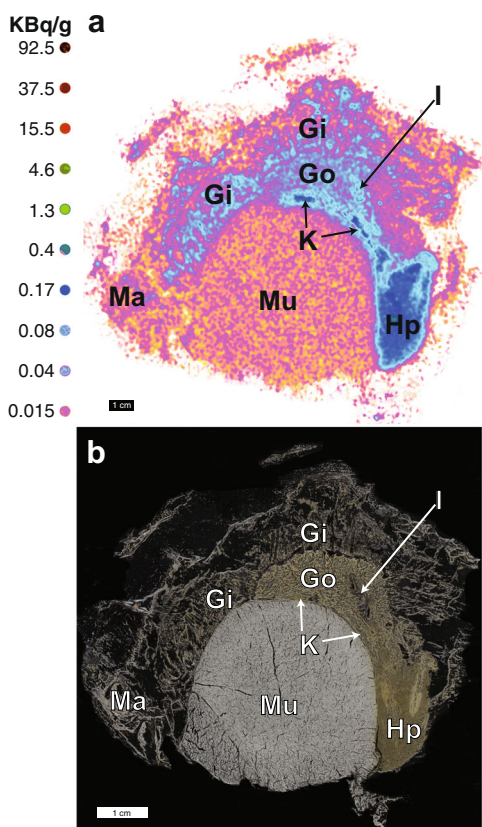
Fig. 3 Quantitative whole-body autoradiography of scallop Pecten maximus. a Autoradiogram and **b** corresponding tissue section of a king scallop (Pecten maximus) showing the typical tissue distributions of radiolabelled nPS observed after a 6-h exposure to waterborne ^{14}C-labelled 20 nm nanoplastic. Colour scales, using standard 16 colours from ImageJ, are in units of kBq/g and differ from one another to illustrate radiolabel distribution in different tissues. Quantified areas on the autoradiogram are displayed in Table 1. Gi gills, Go gonad, Hp hepatopancreas, I Intestine, K kidney, Mu muscle, Ma mantle. The tissue section was 50 μm thick, the exposure time on the phosphor screen was 3 weeks and the scanning resolution was 600 dots per inch (dpi).

[14]C-nPS$_{250}$, respectively. These measurements, as expected, almost certainly overestimated the particle sizes. DLS intensity values tend to overestimate particle size and results are influenced by the few large aggregates and/or clusters that likely occur. The TEM images clearly showed that ~20 nm particles were indeed produced (Fig. 2), but in the absence of surfactant, several clustered and may have been measured as one by DLS, explaining the systematic offset of these data compared to those of the TEM measurements (Fig. 2).

Tissue distribution, quantification, and recovery. We have shown previously the use of two sizes of ^{14}C-nPS in an exposure experiment with king scallops (Pecten maximus) with monitoring of uptake by quantitative whole-body autoradiography (QWBA)[11] to localise the labelled nPS. Without wishing to repeat publish those data, but in order to give further details of the measurement methods, we present additional, unpublished images, from the same experiments herein. Tissue sections were collected in duplicate. The autoradiogram produced from a scallop collected after 6 h exposure to waterborne nominal ^{14}C-nPS$_{20}$ is shown in Fig. 3 and illustrates a tissue distribution typical of the duplicates. Most tissues were labelled (including muscles, gonads, mantle,

gills, intestine and kidney), but the hepatopancreas exhibited the highest ^{14}C concentration.

These and previous data[7] indicate the great advantage of QWBA analysis, viz applicability to the study of anatomical structures, including those which may be very difficult to dissect (e.g. due to their small sizes, their location, or fragility). To achieve such quantitative analyses herein, calibration curves were produced according to a standard operation procedure[11,29] using 20 different screens on which were randomly distributed all the scallop and ^{14}C standard sections (both in CMC gel sections of 50 μm produced by the same procedure using a cryomicrotome). This corresponds to 200 calibration data points. The digital light intensity was plotted against the ^{14}C concentrations of the standard spots. The limits of detection (LOD; $0.19\ Bq\ g^{-1} = 0.28\ ng\ g^{-1} \cong 6.4 \times 10^7\ nPS_{20}$ particles $g^{-1} \cong 3.3 \times 10^4\ nPS_{250}$ particles g^{-1}) and quantification (LOQ; $0.56\ Bq\ g^{-1} = 0.85\ ng\ g^{-1} \cong 1.3 \times 10^8\ nPS_{20}$ particles $g^{-1} \cong 6.5 \times 10^4\ nPS_{250}$ particles g^{-1}) of nPS particles were calculated as corresponding to 3 and 10 times the standard deviations (SD) of the intercepts of the calibration curves, respectively. The phosphor screens used in QWBA are 20 times more sensitive than X-ray films and their linear dynamic range extends over four to five orders of magnitude, allowing capture and quantification of both very low and very high activities, in a single exposure[30]. Quantification data from two scallops per aquarium for three different replicates (i.e. six scallops) for ^{14}C-nPS obtained by QWBA analyses of the different organs (shown in Fig. 3) are given in Table 1. The use of ^{14}C-labelled nPS allowed a mass balance and indicated that recoveries of 81–84% were possible (Table 2). We suspect that the remaining 16.0–18.6% of the ^{14}C-nPS had become incorporated into the faeces or pseudofaeces, or both. One could quantify the amount of particles ending in this compartment, or on the aquarium walls, by collecting them and producing wipes of the walls that could be measured by liquid scintillation counting (LSC).

In summary, a method was developed herein which allowed efficient one-step synthesis of radiolabelled sulfonate end-capped plastic nanoparticles (nPS). Particle synthesis conditions from earlier studies of non-labelled nPS[26,31] were improved in order that only small amounts of expensive isotopically labelled monomers were needed. Also, a better control over nPS sizes was obtained and the method provided ^{14}C-nPS with a specific activity suitable for studies at predicted environmentally relevant concentrations in the parts per billion range[11,12]. As an illustrative example, data showed that waterborne ^{14}C-nPS were readily taken up by the scallop, P. maximus. Autoradiograms revealed a high accumulation of the radiolabelled nPS in the digestive gland. Using QWBA, the quantification of uptake, elimination and biodistribution of plastic particles proved possible, as published in detail elsewhere[11]. The use of a radiotracer also allowed characterisation of the biodistributions in small and fragile organs in the scallop, such as the kidney, anus and intestine. Such detailed distribution images will be highly valuable for improving the understanding of the physiological processes governing the bioaccumulation of micro- and nano-plastics in marine bivalves and other organisms and may help to guide further research work. For example, fundamental biotic and abiotic mechanisms of degradation and assimilation of NP may be studied at environmentally relevant concentrations.

Methods

Chemicals and reagents. Styrene (≥99%, extra pure, stabilised) from ACROS Organics™ was used without purification. Styrene [methylene-14C] in hexane with a specific activity of 2.22 GBq mmol⁻¹ (Mw = 106.14 g mol⁻¹, American radi-olabeled chemicals Inc.) was used as received. Sodium dodecyl sulfate (SDS, ≥99%) obtained from Alfa Aesar™ was used without purification. Potassium persulfate (KPS, ≥99%, ACS reagent) from ACROS organics™ was purified by crystallisation in water. Sodium hydroxide (NaOH, ≥98%) from Honeywell Fulka™. Water used in

Table 1 Quantification of ^{14}C-nPS.

	DLU mm^{-2}	DPM g$_{w.w.}^{-1}$	ng g$_{w.w.}^{-1}$	Bq g$_{w.w.}^{-1}$	Bq	ng	Area (mm^2)	%	g
Hp	58.4 ± 5	9352.6 ± 833	467.6 ± 42	155.9 ± 14	413.8 ± 37	1241.3 ± 111	227.0 ± 39	6.2 ± 1	4.1 ± 0.02
Mu	8.2 ± 0.3	576.1 ± 23	28.8 ± 1	9.6 ± 0.4	226.1 ± 9	678.3 ± 27	1291.1 ± 184	35.0 ± 1	23.5 ± 0.3
K	26.6 ± 6	4174.3 ± 973	208.7 ± 49	69.6 ± 16	86.1 ± 20	258.4 ± 60	67.9 ± 40	1.8 ± 0.4	1.2 ± 0.005
Go	16.5 ± 1	2191.9 ± 185	109.6 ± 9	36.5 ± ± 3	239.4 ± 20	718.3 ± 61	359.4 ± 150	9.7 ± 3	6.6 ± 0.05
Gi	10.6 ± 1	1045.7 ± 94	52.3 ± 5	17.4 ± 2	362.9 ± 33	1088.7 ± 98	1141.8 ± ± 511	30.9 ± 3	20.8 ± 0.6
I	118.5 ± 3	21065.1 + 569	1053.3 ± 28	351.1 ± 9	102.2 ± 3	306.5 ± 8	58.7 ± 21	1.6 ± 0.04	1.1 ± 0.0004
	1273.8 ± 9	38405.6 ± 1417	1920.3 ± 71	640.1 ± 24	1430.5 ± 58	4291.5 ± 173	3145.8 ± 587	85.2 ± 3.3	57.4 ± 0.7

Tissue distribution of ^{14}C-nPS quantified by QWBA after 6-h waterborne exposure ($n = 2$ scallops/aquarium made in triplicate, i.e. with 6 scallops, $n = 120$ sections). *Bg* background, *Gi* gills, *Go* gonad, *Hp* hepatopancreas, *I* intestine, *K* kidney, *Mu* muscle, *DLU* Digital Light Unit, *mm* millimetre, *DPM* disintegration per minute, *Bq* Becquerel, $g_{w.w.}$ grams of wet weight tissues, *ng* nanograms, % percentage.

Table 2 Recovery of ^{14}C-nPS.

		Expected^a		Quantification			
	Burden	per scallop^b	per gram$_{ww}^c$	QWBA^d	per gram$_{ww}^c$	Recovery	Loss
μg	78 ± 15.6	6.5 ± 1.3	0.089 ± 0.03	4.3 ± 0.2	0.075 ± 0.02	84 ± 28%	16 ± 33%
ng	78,000 ± 15,600	6500 ± 1300	89.0 ± 29	4291.5 ± 173	74.8 + 25	84 ± 28%	16 ± 33%
Bq	30,000 ± 6000	2500 ± 500	34.25 ± 11	1650 ± 64	27.9 ± 9	84 ± 28%	16 ± 33%

Burden of ^{14}C-nPS per scallop and per wet weight gram of tissue and ^{14}C-nanopolytyrene recovery following exposure experiments.
^{a}Calculated for an average of 73 ± 24 g per scallops.
^{b}12 scallops per tank.
^{c}Per gram wet weight.
^{d}Quantification from the QWBA for the scallops quantified in Fig. 3.

synthesis was purified with Milli-Q® Integral Water Purification System for Ultrapure Water (18.2 MΩ cm^{-1}).

Synthesis (Supplementary Table 3). The synthesis was developed and each chemical that could influence the polymerisation by emulsion tested in experiments named as follows: Experiment 1 (Exp 1): all tests related to 20 nm nPS (nPS$_{20}$); Experiment 2 (Exp 2): all tests related to 250 nm nanopolystyrene (nPS$_{250}$); Experiment 3 (Exp 3) radiolabeled nPS$_{20}$ and nPS$_{250}$.

Synthesis of nPS$_{20}$ (Exp 1) was first optimised without radioactivity following the method proposed by Ming et al.[31]. nPS$_{20}$ was prepared by dropwise addition of styrene into the SDS/H$_2$O system at room temperature and polymerised in a three-necked flask under a pure nitrogen atmosphere to complete conversion at 70 °C. The solution turned white with the formation of nPS when synthesis was complete.

The initial synthesis (Exp 1.1) was a conventional emulsion system with styrene 7.8 wt%, SDS 2 wt%, water 90.2 wt%, and KPS 3.6 mM was also polymerised at 70 °C.

In a second step (Exp 1.2), to assess the impact of the limiting amount of ^{14}C-styrene on the particles size, the concentration of styrene (Δ[Sty]) was considered. Consequently, styrene was decreased from 7.8% to 1 wt% (i.e. 7.8, 5, 3, 2, 1 wt%). Emulsion system was fixed with water 90.2 wt%, SDS 2 wt% and KPS 3.6 mM at 70 °C.

In a third step (Exp 1.3), several concentrations of the initiator KPS (Δ[KPS]) were tested as the following: 0.5, 1, 3.6, 14.6, 50 mM with the emulsion system fixed at styrene 1 wt%, SDS 2 wt% and water 90.20 wt% at 70 °C.

In a fourth step (Exp 1.4), the effect of SDS concentration (Δ[SDS]) on particles size were tested at 0.5, 1, 2, 3 wt% with the emulsion system fixed at styrene 1 wt%, water 90.20 wt% and KPS 3.6 mM at 70 °C.

Two hundred and fifty nanometre nPS (nPS$_{250}$) synthesis (Exp 2) is a surfactant-free synthesis. nPS$_{250}$ was prepared by dropwise addition of styrene into the NaOH/H$_2$O system at room temperature and polymerised in a three-necked flask under a pure nitrogen atmosphere to complete conversion at 70 °C. The solution turned white with the formation of nPS when synthesis was complete.

In a first step (Exp 2.1), nPS$_{250}$ was prepared by surfactant-free emulsion polymerisation adapted from Telford et al.[26]. In the surfactant-free emulsion polymerisations, styrene 20 wt% and Milli-Q water 59 wt% were mixed at room temperature in a 50 mL round-bottom flask. The flask was sealed with a rubber septum. The headspace inside the flask was then quickly purged with nitrogen for 30 s. The flask was immersed in a silicon oil bath at 70 °C for 5 min, with stirring. In the meanwhile, initiator solution was prepared separately with KPS 3 wt% (14.6 mM in the final water phase), NaOH 2 wt% (56.7 mM in the final phase), and Milli-Q water 17 wt% were mixed in a glass vial. Once the round-bottom flask medium reached 70 °C, the initiator solution was injected in the round-bottom flask through the rubber septum, using a syringe. The reaction mixture was vigorously stirred at 70 °C overnight.

In a second step (Exp 2.2), to assess the impact of the limiting amount of ^{14}C-styrene on particle size, the concentration of styrene (Δ[Sty]) was considered. Concentrations tested were 1, 2, 3, 5 and 20%. The system was fixed with NaOH 2 wt%, water 76 wt% and KPS 14.6 mM at 70 °C.

In a third step (Exp 2.3), several concentrations of the initiator KPS (Δ[KPS]) were tested as the following: 0.07, 2.7, 14.6 and 50 mM. The system was fixed with styrene 1 wt%, NaOH 2 wt% and water 76 wt% at 70 °C.

Radiolabeling synthesis of 20 and 250 nm nPS (Exp 3) used the optimised parameters from Exp 1 and 2. For comparison both size target and radiolabeling purpose, styrene proportion was decreased at 1 wt% and the volume of synthesis at 10 mL. Both synthesised, the reactions were mixture was vigorously stirred at 70 °C overnight.

Radiolabeled 20 nm nPS (^{14}C-nPS$_{20}$) was prepared (Exp 3.1) by a conventional emulsion system with styrene 1 wt%, SDS 2 wt%, water 90.20 wt%, and KPS 3.60 mM in a 40-mL vial closed with a rubber cap. The vial was purged with nitrogen gas for 30 s and then heated at 70 °C. Once 70 °C was reached, ^{14}C-styrene was a dropwise addition with a syringe. The solution turned white with the formation of nPS when synthesis is successful.

Radiolabeled 250 nm nPS (^{14}C-nPS$_{250}$) was prepared (Exp 3.2) by a surfactant-free emulsion polymerisations. The initiator solution was prepared separately with KPS 3 wt% (14.6 mM in the final water phase), NaOH 2 wt% (56.7 mM in the final water phase), and Milli-Q water 17 wt% were mixed in a glass vial. Styrene 1 wt% and Milli-Q water 59 wt% were mixed at room temperature in a 40 mL vial. The vial was sealed with a rubber septum. The headspace inside the flask was then purged with nitrogen for 30 s. The vial was immersed in a silicon oil bath at 70 °C for 5 min, with stirring. In the meanwhile, Once the vial medium reached 70 °C, the initiator solution was injected through the rubber septum, using a syringe.

Purification of PS latexes. All chemicals unreacted were systematically removed by ultrafiltration (exclusion size of membrane: 30,000 g mol^{-1}) with a dialysis membrane. Water was frequently changed for 48 h, until the conductivity of water remained constant at a value of <1.5 μS cm^{-1}.

DLS, surface charge (ζ-potential) (Supplementary Table 1). After completion of the polymerisation reaction, the l hydrodynamic diameters of the lattices were characterised in water at 20 °C. The average sizes and ζ-potentials of the polymer particles were measured using a multi-angle Nicomp ZLS Z3000 (Particle Sizing System, Port Richey, FL). DLS measurements give a value called Z-average size (or cumulative mean), which is an intensity mean, and the polydispersity index. The latex dispersions are optimised for the DLS measurements by diluting the crude, concentrated, reaction product with an excess of Milli-Q water until the count rate of the resulting mixture is within the optimal range. The final concentrations were typically about 1 mg L^{-1} and can be estimated from the concentration of the primary emulsion. Each sample was analysed at least five times.

Transmission and scanning electronic microscopy (TEM, STEM) (Supplementary Figs. 1 and 2 and Table 2). All particle morphology and size measurements were recorded with a JEOL JEM-1400 transmission electron microscope at Plymouth Electron Microscopy Centre (PEMC, University of Plymouth, United Kingdom, operated at an acceleration voltage of 80 kV) and with a scanning transmission electron microscope (STEM, HD-2700-Cs, Hitachi, Japan, ETH Zurich, operated at an acceleration voltage of 200 kV). Samples were prepared and dried at ambient temperature under a laminar flow fume hood. Each latex sample was diluted to about 0.01% solid content and a drop was placed onto a carbon-coated copper grid 200 mesh. Grids were then rinsed five times in five different drops of Milli-Q water. Grids were kept in a desiccator cabinet to remove all humidity overnight. Additional contrasting agents were not applied. At least 10 TEM images were obtained from at least 10 different areas on each grid. The diameters of at least 100 particles in each sample were determined on TEM images recorded using ImageJ software (open source, https://imagej.nih.gov/ij/).

Fourier transform infrared (FTIR) spectroscopy (Supplementary Fig. 3). The polymers were characterised by FTIR spectroscopy (Alpha FTIR, Brucker) working in Attenuated Total Reflectance (ATR) mode with a DTGS detector. Spectra were recorded with 16 scans at $4\,cm^{-1}$ resolution, covering the spectral range between 4000 and $600\,cm^{-1}$. FTIR measurements were performed to confirm polymerisation success and library spectral matching was used to identify each product.

Yield determinations. To assess synthesis yields, all masses were measured before and after synthesis for the cold synthesis. Comparison with the yields of the radiolabeled synthesis were made by measuring radioactivity before synthesis and after the purification step.

Scallop exposure design. In a preliminary experiment aimed at verifying the usefulness of radiolabeled nPS for bioaccumulation studies, a group of 12 king scallops (*P. maximus*) were exposed to a waterborne ^{14}C-nPS (0.3 MBq mg^{-1} ^{14}C, $t_{1/2} = 5700$ y, β-emitter) at 5 kBq L^{-1} (15 μg L^{-1} ^{14}C) for 6 h. Seawater (20 L) was filtered on a sand filter. Water temperature was maintained at 12–13 °C and kept oxygenated by air bubbling. The salinity of the seawater was 32 psu and the pH was stable at 8.0.

Liquid scintillation counting. ^{14}C activity was measured by an Hidex 300SL counter at the University of Cambridge, Gordon institute facilities (10 min counting time, minimum detectable activity 0.08 Bq ml^{-1}). Synthesis yield was assessed by measuring the ^{14}C activity at the addition of ^{14}C-styrene and after ultrafiltration purification (cut-off, 8 kDa).

Quantitative whole-body autoradiography. At the end of the exposure period, scallop soft tissues were removed from the shell and used for QWBA. Briefly, tissues were included in a carboxylmethylcellulose gel and frozen in liquid nitrogen. From the resulting block, 20 pairs of 50-μm-thick sections were sampled at −25 °C with a Leica CM3600 cryomicrotome. Sections were freeze-dried for 36 h at −25 °C, exposed on phosphor screens sensitive to beta radiation for 1 week and scanned with a Typhoon FLA7000 from GE Healthcare to reveal the autoradiograms. Radiolabel concentrations in tissues were quantified from the images obtained with ImageJ as Digital Light Unit (DLU) per mm^2 and transformed into ng/g using a calibration blood spot on each screen.

Sectioning. Cross-contamination was avoided as there was no direct manipulation of organs and tissues and the only instrument coming into contact with them was the microtome knife, which was carefully cleaned with a brush before every section.

Data availability

All data generated or analysed during this study are included in this published article (and its supplementary information files).

References

1. Klaine, S. J. et al. Paradigms to assess the environmental impact of manufactured nanomaterials. *Environ. Toxicol. Chem.* **31**, 3–14 (2012).
2. Koelmans, A. A., Besseling, E. & Shim, W. J. in *Marine Anthropogenic Litter* (eds Bergmann, M. et al.) 325–340 (Springer International Publishing, 2015).
3. Gangadoo, S. et al. Nano-plastics and their analytical characterisation and fate in the marine environment: from source to sea. *Sci. Total Environ.* **732**, 138792 (2020).
4. Hernandez, L. M., Yousefi, N. & Tufenkji, N. Are there nanoplastics in your personal care products? *Environ. Sci. Technol. Lett.* **4**, 280–285 (2017).
5. Hernandez, L. M. et al. Plastic teabags release billions of microparticles and nanoparticles into tea. *Environ. Sci. Technol.* https://doi.org/10.1021/acs.est.9b02540 (2019).
6. Lambert, S., Sinclair, C. J., Bradley, E. L. & Boxall, A. B. A. Effects of environmental conditions on latex degradation in aquatic systems. *Sci. Total Environ.* **447**, 225–234 (2013).
7. Lambert, S. & Wagner, M. Characterisation of nanoplastics during the degradation of polystyrene. *Chemosphere* **145**, 265–268 (2016).
8. Gigault, J., Pedrono, B., Maxit, B. & Ter Halle, A. Marine plastic litter: the unanalyzed nano-fraction. *Environ. Sci. Nano* **3**, 346–350 (2016).
9. Tian, L. et al. A carbon-14 radiotracer-based study on the phototransformation of polystyrene nanoplastics in water versus in air. *Environ. Sci. Nano* **6**, 2907–2917 (2019).
10. Chae, Y. & An, Y.-J. Effects of micro- and nanoplastics on aquatic ecosystems: current research trends and perspectives. *Mar. Pollut. Bull.* **124**, 624–632 (2017).
11. Al-Sid-Cheikh, M. et al. Uptake, whole-body distribution, and depuration of nanoplastics by the scallop Pecten maximus at environmentally realistic concentrations. *Environ. Sci. Technol.* **52**, 14480–14486 (2018).
12. Lenz, R., Enders, K. & Nielsen, T. G. Microplastic exposure studies should be environmentally realistic. *Proc. Natl Acad. Sci. USA* **113**, E4121–E4122 (2016).
13. Ward, J. E. & Kach, D. J. Marine aggregates facilitate ingestion of nanoparticles by suspension-feeding bivalves. *Mar. Environ. Res.* **68**, 137–142 (2009).
14. Bhattacharya, P., Lin, S., Turner, J. P. & Ke, P. C. Physical adsorption of charged plastic nanoparticles affects algal photosynthesis. *J. Phys. Chem. C* **114**, 16556–16561 (2010).
15. Lee, K.-W., Shim, W. J., Kwon, O. Y. & Kang, J.-H. Size-dependent effects of micro polystyrene particles in the marine copepod Tigriopus japonicus. *Environ. Sci. Technol.* **47**, 11278–11283 (2013).
16. Ma, Y. et al. Effects of nanoplastics and microplastics on toxicity, bioaccumulation, and environmental fate of phenanthrene in fresh water. *Environ. Pollut.* **219**, 166–173 (2016).
17. Mattsson, K. et al. Brain damage and behavioural disorders in fish induced by plastic nanoparticles delivered through the food chain. *Sci. Rep.* **7**, 11452 (2017).
18. Moestue, S. et al. Whole-body section fluorescence imaging—a novel method for tissue distribution studies of fluorescent substances. *Contrast Media Mol. Imaging* **4**, 73–80 (2009).
19. Catarino, A. I., Frutos, A. & Henry, T. B. Use of fluorescent-labelled nanoplastics (NPs) to demonstrate NP absorption is inconclusive without adequate controls. *Sci. Total Environ.* **670**, 915–920 (2019).
20. Abdurahman, A. et al. Adsorption of dissolved organic matter (DOM) on polystyrene microplastics in aquatic environments: kinetic, isotherm and site energy distribution analysis. *Ecotoxicol. Environ. Saf.* **198**, 110658 (2020).
21. Khan, A. Y., Talegaonkar, S., Iqbal, Z., Ahmed, F. J. & Khar, R. K. Multiple emulsions: an overview. *Curr. Drug Deliv.* **3**, 429–443 (2006).
22. Thickett, S. C. & Gilbert, R. G. Emulsion polymerization: state of the art in kinetics and mechanisms. *Polymer (Guildf)* **48**, 6965–6991 (2007).
23. Yamamoto, T. & Higashitani, K. Growth processes of poly methylmethacrylate particles investigated by atomic force microscopy. *Adv. Powder Technol.* **18**, 567–577 (2007).
24. Chern, C. S. Emulsion polymerization mechanisms and kinetics. *Prog. Polym. Sci.* **31**, 443–486 (2006).
25. Anderson, C. D. & Daniels, E. S. *Emulsion Polymerisation and Latex Applications* (Rapra Technology, 2003).
26. Telford, A. M., Pham, B. T. T., Neto, C. & Hawkett, B. S. Micron-sized polystyrene particles by surfactant-free emulsion polymerization in air: synthesis and mechanism. *J. Polym. Sci. A Polym. Chem.* **51**, 3997–4002 (2013).
27. Erickson, H. P. Size and shape of protein molecules at the nanometer level determined by sedimentation, gel filtration, and electron microscopy. *Biol. Proced. Online* **11**, 32–51 (2009).
28. Chen, J. et al. Polystyrene/MMT nanocomposites prepared by soap-free emulsion polymerization with high solids content. *Colloid Polym. Sci.* **290**, 1955–1963 (2012).
29. Al-Sid-Cheikh, M., Rouleau, C., Bussolaro, D., Oliveira Ribeiro, C. A. & Pelletier, E. Tissue distribution of radiolabeled 110m Ag nanoparticles in fish: Arctic Charr (Salvelinus alpinus). *Environ. Sci. Technol.* **53**, 12043–12053 (2019).
30. L'Annunziata, M. F. *Handbook of Radioactivity Analysis.* https://doi.org/10.1016/B978-0-12-436603-9.X5000-5 (2003).
31. Ming, W., Zhao, J., Lu, X., Wang, C. & Fu, S. Novel characteristics of polystyrene microspheres prepared by microemulsion polymerization. *Macromolecules* **29**, 7678–7682 (1996).
32. Ronco, L. I., Minari, R. J. & Gugliotta, L. M. Particle nucleation using different initiators in the microemulsion polymerization of styrene. *Brazilian J. Chem. Eng.* **32**, 191–200 (2015).

33. Berber, H. Emulsion polymerization: effects of polymerization variables on the properties of vinyl acetate based emulsion polymers. *Polym. Sci.* https://doi.org/10.5772/51498 (2013).

Acknowledgements

Author contributions

M.A.-S.-C., S.J.R., R.C.T. and T.B.H. planned and designed the research. M.A.-S.-C. performed the radiolabelling, histological preparations and analytical measurements. M.A.-S.-C. and M.-A.C. performed exposure experiments and sample preparation. M.A.-S.-C. analysed data. M.A.-S.-C. and R.K. performed T.E.M. and S.E.M. and analysed images. M.A.-S.-C., S.J.R., R.C.T., T.B.H., R.K. and M.-A.C. wrote the manuscript.

Competing interests

The authors declare no competing interests.

Additional information

Supplementary information is available for this paper at https://doi.org/10.1038/s43246-020-00097-9.

Correspondence and requests for materials should be addressed to M.A.-S-C.

Peer review information Primary handling editor: John Plummer.

Reprints and permission information is available at http://www.nature.com/reprints

Publisher's note Springer Nature remains neutral with regard to jurisdictional claims in published maps and institutional affiliations.